IEEE Robotics and Automation Letters (RA-L) paper, presented at ICRA 2026, Vienna, Austria. Cite as RA-L paper.

Enhancing Motor Synchrony in Rhythmic Dyadic Tasks Through Portable Elbow Exoskeletons

Emanuele Peperoni, Stefano Laszlo Capitani, Lorenzo Grazi, *Member, IEEE*, Michele Francesco Penna, Lorenzo Amato, Filippo Dell'Agnello, Andrea Baldoni, Domenico Formica, *Senior Member, IEEE*, Marc Leman, Nicola Vitiello, *Member, IEEE*, Simona Crea, and Emilio Trigili, *Member, IEEE*

***Abstract*—Synchrony is a cornerstone for the successful physical interaction between humans while cooperating or competing towards a goal and is achieved by correct and smooth information exchange between subjects. Recently, Human-Robot-Human (HRH) interaction arose as an emerging paradigm for improving motor control in collaborative and dyadic motor tasks. Among the robotic solutions explored for agent coupling, exoskeletons are powerful tools for exerting torque and force feedback at the joint level. In this work, two identical torque-controlled elbow exoskeletons were used in dyadic interaction, to provide haptic feedback and improve synchrony between two individuals performing a tapping task. Each exoskeleton is lightweight and compact, weighing 0.8 kg on the arm. Bench tests to verify the performance of closed-loop torque control showed a residual torque below 0.2 Nm when the reference torque was set to zero, and a bandwidth higher than 6 Hz, thus achieving adequate performance for applications in HRH scenarios. In human subjects' experiments, the root-mean-squared error between the two users' joint trajectories was 50% lower when users received haptic feedback compared to the condition without feedback; the relative phase error was lower than 60%. The results of this study suggest that exoskeletons can enhance synchrony in HRH interactions, being potentially useful in rehabilitation training, collaborative industrial tasks or sport and music learning.**

***Index Terms*—Haptics and haptic interfaces, physical human-robot interaction, wearable robotics.**

Received 20 February 2025; accepted 12 July 2025. Date of publication 11 August 2025; date of current version 26 August 2025. This article was recommended for publication by Associate Editor M. Selvaggio and Editor K. Kyung upon evaluation of the reviewers' comments. This work was supported by the European Commission through H2020 under Grant CONBOTS ICT 871803. *(Emanuele Peperoni and Stefano Laszlo Capitani contributed equally to this work.) (Corresponding author: Emilio Trigili.)*

This work involved human subjects or animals in its research. Approval of all ethical and experimental procedures and protocols was granted by the Joint Ethics Committee of Scuola Superiore Sant'Anna and Scuola Normale Superiore under Application No. 39/2023, and performed in line with the Declaration of Helsinki.

Emanuele Peperoni, Stefano Laszlo Capitani, Lorenzo Grazi, Michele Francesco Penna, Lorenzo Amato, Filippo Dell'Agnello, Andrea Baldoni, Nicola Vitiello, Simona Crea, and Emilio Trigili are with the The BioRobotics Institute, Scuola Superiore Sant'Anna, 56025 Pontedera, Italy, and also with the Department of Excellence in Robotics and AI, Scuola Superiore Sant'Anna, 56127 Pisa, Italy (e-mail: emilio.trigili@santannapisa.it).

Domenico Formica is with the Neurorobotics Lab, Newcastle University, NE1 7RU Newcastle upon Tyne, U.K., and also with the NEXT: Neurophysiology and Neuroengineering of Human-Technology Interaction Research Unit, Università Campus Bio-Medico di Roma, 00128 Rome, Italy.

Marc Leman is with the Faculty of Arts and Philosophy, IPEM Institute of Psychoacoustics and Electronic Music, University of Ghent, 9000 Gent, Belgium.

This article has supplementary downloadable material available at https://doi.org/10.1109/LRA.2025.3597511, provided by the authors.

Digital Object Identifier 10.1109/LRA.2025.3597511

I. Introduction

When humans collaborate or compete task execution, spatial and temporal relations between the agents (i.e., humans) are relevant for successful task completion [1]. Especially for tasks like precise joint manipulation or goal-directed pick and place, synchrony plays a fundamental role [2]. Synchrony refers to the temporal alignment in period or phase between individuals performing repetitive actions [3]. This relation is assumed to be controlled by predictive models that use information coming from different sensory channels, and it and is essential for tasks ranging from simple tapping to complex arm movements [2]. Information exchange during such tasks typically relies on visual or auditory cues. Studies have explored enhancing human performance by augmenting these sensory channels with additional task-relevant information [4]. Recently, haptic feedback during human-human interaction has been shown to improve the task performance and the individual motor learning of the involved agents [5]. Vibrotactile stimulation provided via eccentric motors embedded in bands and belts has been shown to improve performance in sports and dance, particularly during simple exercises, although it is challenging to develop a meaningful yet informative stimulus for complex tasks [6]. On the other hand, joint-torque feedback provides an intuitive, movement-related information that can be exploited by the user in the motor task [7]. Despite its neurophysiological advantages, such as a shorter sensory pathway linking external input to perception, there is still a lack of strong evidence supporting the prevalence of the haptic interaction over visual feedback in joint coordination tasks between users [8], [9]. Robotic devices can provide haptic feedback to paired individuals, enabling them to physically interact despite being spatially distant or separated, a concept known as Human-Robot-Human (HRH) interaction [10]. Two main architectures of robots have been adopted depending on the application scenarios, namely end-effector devices and wearable robots. End-effector robots can integrate high-power actuation units with high performance in closed-loop force/torque control [11]. The haptic information can be rendered only at the endpoint [12], posing some limitations when tested in tasks that simulate daily-life activities. Conversely, wearable robots can render forces and torques at joint level, supporting free 3D movements and complex multi-joint tasks while delivering haptic feedback enriched with kinematic information about the movement [13]. Some recent works attempted to investigate the role of haptic feedback via lower-limb exoskeletons during HRH interaction, both on single-joint movements and in more complex tasks such as sit-to-stand transitions [14], [15]. However, applications

2377-3766 © 2025 IEEE. All rights reserved, including rights for text and data mining, and training of artificial intelligence and similar technologies. Personal use is permitted, but republication/redistribution requires IEEE permission. See https://www.ieee.org/publications/rights/index.html for more information.

©2026 IEEE

Authorized licensed use limited to: Scuola Superio Sant'Anna di Pisa. Downloaded on August 27,2025 at 06:59:11 UTC from IEEE Xplore. Restrictions apply.

IEEE Robotics and Automation Letters (RA-L) paper, presented at ICRA 2026, Vienna, Austria. Cite as RA-L paper.

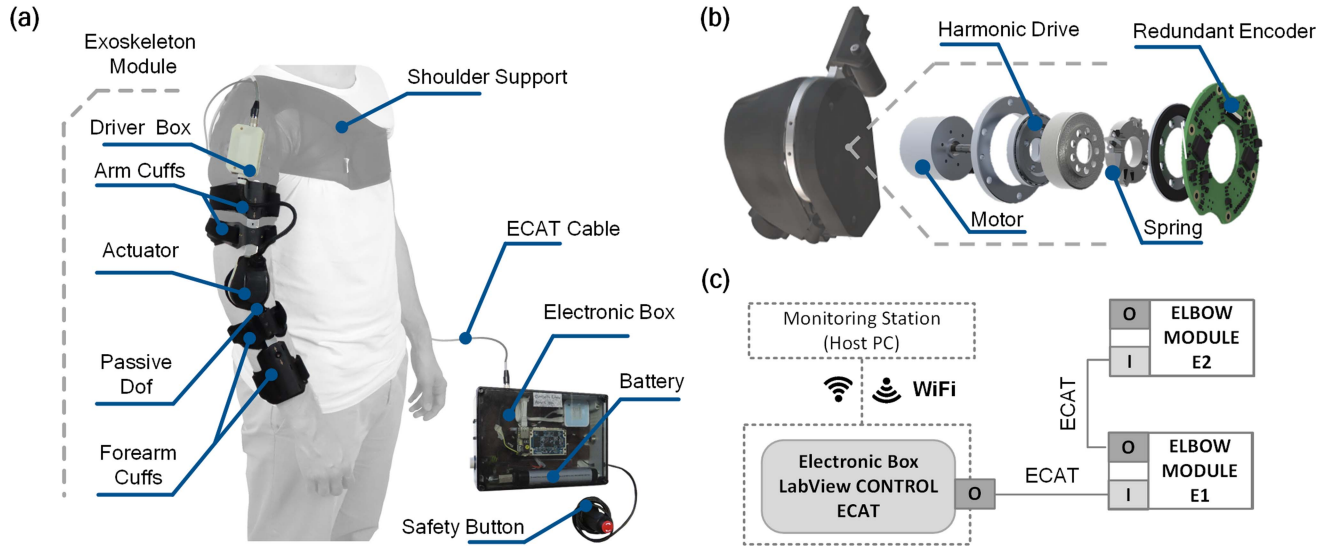

Fig. 1. Overview of the system. (a) The exoskeleton module and electronic box. (b) Exploded view of the components of the series elastic actuator. (c) Communication scheme between the electronic box, two elbow exoskeletons and the monitoring station.

involving upper-limb exoskeletons remain limited. Some research has explored visuomotor tasks in rehabilitation settings [16]. Despite their potential to enhance HRH interactions in everyday activities, sports, and music, designing upper-limb exoskeletons that balance portability and torque tracking performance remains challenging. Weight and bulkiness are major factors affecting user acceptance and potentially hampering the feedback effectiveness [17]. Additionally, haptic feedback must be precisely modulated to be effectively incorporated into motor patterns, requiring high torque resolution and bandwidth [18]. To address these requirements, Series-Elastic-Actuators (SEAs) represent a viable solution to achieve (i) a closed-loop torque control (ii) smooth and safe interaction and (iii) visco-elastic behavior adaptable to different interaction paradigms [19].

This letter presents a compact, lightweight SEA-based elbow exoskeleton designed to provide haptic feedback in HRH interaction between physically unimpaired individuals. The elbow joint was chosen due to its key role in hand positioning and controlling the timing of upper-limb gestures [20], which are relevant for studying synchronization between agents, especially in leisure activities such as music playing with drums or violins, sports or dance [21]. The following sections discuss the device requirements, mechatronic implementation, and characterization. The experimental validation focuses on evaluating the impact of haptic feedback to improve synchrony between users in a dyadic task.

II. Exoskeleton Prototype

A. Design Requirements

In unimpaired individuals performing daily activities, the elbow joint has a range of motion (RoM) spanning from 0 to 130 deg, with a maximum speed of 330 deg/s. Movement frequencies within this RoM can reach up to 3 Hz [22], with an expected average of 1.2 Hz [23]. In addition, the minimum perceivable torque at the elbow is 0.2 Nm in static conditions and 0.8-1 Nm during dynamic tasks [24]. The maximum biological elbow torque is below 3 Nm in daily tasks that do not entail the manipulation of external loads [25]. Based on the aforementioned data, the exoskeleton was designed to fit physiological movement angles and speed, with a minimum output torque resolution of 10 mNm and a peak torque of 4.5 Nm [23]. Particular attention was given to designing a system with an overall weight below 1.2 kg and with limited encumbrance, considering that these features are paramount for device acceptability [26].

The developed system is a Portable Elbow acTive Exoskeleton (PETE) (Fig. 1). PETE comprises a wearable exoskeletal module and an electronic box located remotely, as this configuration reduces the weight on the user. The wearable module can be adjusted to fit the right or left arm and is made of two main components: (i) the actuation unit, and (ii) the physical human-robot interface (pHRI). In this work, two exoskeletal modules are used in a dyadic task.

B. Actuation Unit

The selection of the actuator's components followed the procedure presented in [27]. The working cycle of the actuation unit consisted of sinusoidal F/E movements within the physiological RoM and speed, and an output torque of 6 Nm at the speed peak. The motor, reducer and spring were selected to minimize the overall encumbrance while ensuring that the current saturation and maximum speed limits of the motor were not reached within the working cycle. The designed actuation unit is a Force Sensing Series Elastic Actuation (FSEA) [19]. The FSEA integrates an electric motor, a reduction stage, and a custom torsional spring [28]. A brushless DC-Flat motor (3216 024 BXT H, Faulhaber, Schönaich, Germany) delivers 20 W of power at 24 V. The reduction stage is a Harmonic Drive (CSD14802AGR, Harmonic Drive SE, Germany) with an 80:1 reduction ratio. Spring stiffness was selected iteratively by FEM simulation to achieve a peak torque higher than 4.5 Nm while ensuring at least a resolution of 10 mNm for precise control, considering a minimum encoder resolution of 16 bits. The final design of the torsional spring has a stiffness of 138 Nm/rad and can reach a

Authorized licensed use limited to: Scuola Superio Sant'Anna di Pisa. Downloaded on August 27,2025 at 06:59:11 UTC from IEEE Xplore. Restrictions apply.

IEEE Robotics and Automation Letters (RA-L) paper, presented at ICRA 2026, Vienna, Austria. Cite as RA-L paper.

maximum torque peak of up to 7 Nm before damage. The spring deflection is measured using a single magnetic encoder with a double magnetic head configuration (MB039, RLS AksIM-2 redundant, Ljubljana, Slovenija), enabling torque measurement with a resolution of 6.6 mNm. The encoder is also used to measure the elbow joint angle. The resulting actuation unit has compact dimensions (87x64x66 mm) and weighs 0.4 kg.

C. Physical Human-Robot Interface

The pHRI is composed of two main components, namely (i) an elbow orthosis and (ii) a shoulder support vest. The elbow orthosis is customized from a commercial elbow brace (Innovator X, Össur, Reykjavik, Iceland). Two couples of C-shaped cuffs are used to attach the orthosis' links to the upper arm and forearm, respectively, through Velcro straps. These cuffs are padded with soft material and can be easily adjusted to conform to the human limbs. To accommodate different arm lengths, both distances between the two upper-arm cuffs and the two forearm cuffs can be adjusted. A rotational passive joint is integrated in the forearm link, with its rotation axis perpendicular to the elbow rotation axis and the forearm link, to leave the wrist pronation-supination movement free. The shoulder support vest (ACT-100 DX, FGP s.r.l, Verona, Italy) prevents the exoskeleton from slipping along the user's arm during operation. The overall weight of the pHRI is 0.4 kg, hence the overall weight of the device is 0.8 kg.

D. Electronics

The remote electronic box comprises: (i) a custom control board endowed with a commercial system on module (SbRIO-9651, National Instruments, Austin, Texas, USA), embedding a Zynq-7020 FPGA and a LinuxRT real-time processor, (ii) a WiFi nano router for interfacing with an external laptop, and (iii) a LiIon battery (Li-Ion, 8 cells, 28.8 V – 2250 mAh, Inspired Energy, Kirkham, U.K.). The EtherCAT (ECAT) protocol is used to connect the motor driver (Platinum Solo Twitter 15/100, Elmo Motion Control Ltd., Petach-Tikva, Israel) to the control electronics. The driver box includes a low noise fan for heat dissipation. ECAT communication also enables real-time monitoring of parameters like thermal output, providing an overheat safety measure. The control electronics can drive one exoskeleton module (E1) or both (E1 and E2) simultaneously. In this case, an additional cable for ECAT communication connects the E1 and E2 motor drivers, so that the two modules are operated synchronously. The box acts as master of the communication, while the two modules are slaves.

E. Control Architecture and Strategies

The control architecture is based on a three-layer hierarchical structure, namely low-, middle-, and high-level control layers (Fig. 2). The *low-level control* runs on the FPGA at 500 Hz. It implements a closed-loop torque compensator, which sets the reference current to the motor driver based on the difference between the desired and measured torques (τ_{des}, τ_{meas}). The controller is a lead-lag compensator designed via a pole placement method, based on the identification of the open-loop transfer function [19]. The *middle-level control* runs on the RT processor at 100 Hz and computes the τ_{des} according to a virtual impedance paradigm (1):

$$\tau_{des} = K_v\ (\theta_{des} - \theta_{meas}) - B_v\dot{\theta}_{meas} \tag{1}$$

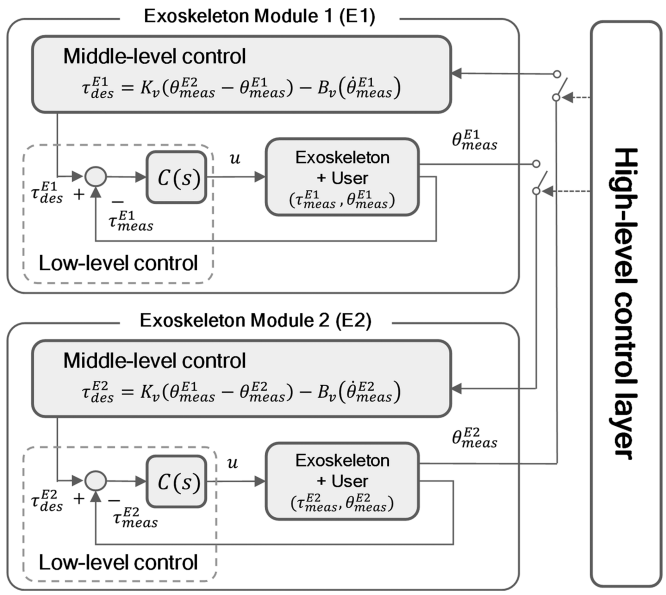

Fig. 2. Control scheme for the human-robot-human interaction. E1 and E2 are the two exoskeleton modules. The high-level control layer sets the desired interaction paradigm between the subjects. In the *bidirectional interaction,* the middle-level control sets the desired angle of each module as the measured angle of the opposite one. In the *unidirectional interaction*, the same control scheme is applied, but one of the two exoskeletons is operating in *transparent mode* ($\boldsymbol{\tau_{des}} = 0$). In the *no interaction* paradigm, both exoskeletons are in *transparent mode*.

where K_v and B_v are set as virtual stiffness and damping coefficients, respectively, and θ_{des} and θ_{meas} are the desired and measured elbow angles, respectively, and $\dot{\theta}_{meas}$ is the measured velocity (estimated from angle differentiation). In the presented application, the virtual stiffness K_v was set to 2.7 Nm/rad while the damping term B_v was set to 0.23 Nms/rad, resulting in a maximum output torque of 5.65 Nm at the joint level in case of deviation from an equilibrium point (assuming a range of motion 0 -120 deg). The damping term B_v was included to ensure stability of the control law, which does not consider the difference between users' speed, as accounted in other studies [7], [14]. The *high-level control* runs on the RT processor, and it is used to manually set the HRH interaction paradigm among the following:

1) No interaction (NI): the E1 and E2 exoskeletons are controlled in the so-called transparent mode (TM), in which $\boldsymbol{\tau_{des}^{E1}} = \boldsymbol{\tau_{des}^{E2}} = 0$ Nm; in this condition, the users can move freely without receiving any haptic feedback.
2) Unidirectional interaction (UI): the E1 (or E2) exoskeleton operates in TM, while the E2 (or E1) provides a desired torque according to (1), where $\boldsymbol{\theta_{des}} = \boldsymbol{\theta_{meas}^{E1}}$ and $\boldsymbol{\theta_{meas}} = \boldsymbol{\theta_{meas}^{E2}}$ (or vice versa). In this way, the user of E1 (or E2) acts as the leader, moving freely and driving the user of E2 (or E1), the follower, toward his/her kinematic trajectory.
3) Bidirectional interaction (BI): both modules are controlled to create a virtual coupling between the users, as in (2) and (3):

$$\tau_{des}^{E1} = K_v\ \left(\theta_{meas}^{E2} - \theta_{meas}^{E1}\right) - B_v\dot{\theta}_{meas}^{E1} \tag{2}$$

$$\tau_{des}^{E2} = K_v\ \left(\theta_{meas}^{E1} - \theta_{meas}^{E2}\right) - B_v\dot{\theta}_{meas}^{E2} \tag{3}$$

Authorized licensed use limited to: Scuola Superio Sant'Anna di Pisa. Downloaded on August 27,2025 at 06:59:11 UTC from IEEE Xplore. Restrictions apply.

IEEE Robotics and Automation Letters (RA-L) paper, presented at ICRA 2026, Vienna, Austria. Cite as RA-L paper.

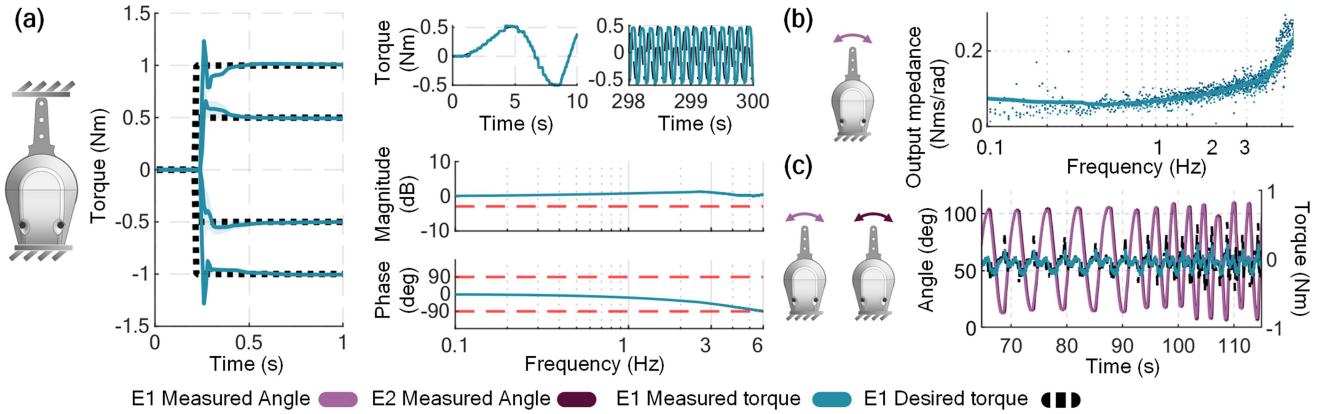

Fig. 3. Bench-top characterization of the actuation unit. Both step and chirp signal are shown removing the offset at mechanical end-stop. (a) Step response analysis for both flexion and extension and bandwidth analysis of the descriptive transfer function $\boldsymbol{H(s) = \tau^{SEA}_{meas}(s)/\tau^{SEA}_{des}(s)}$. (b) Magnitude of the estimated output impedance $\boldsymbol{Z(s) = \tau^{SEA}_{meas}(s)/\dot{\theta}(s)}$ for the frequency range explored (c) Results for the haptic rendering performance, where E1 was driven in impedance control following the trajectory imposed on E2 by a user.

III. Bench-Top Characterization

Step and chirp response characterization was conducted to evaluate the system responsiveness and the torque bandwidth, respectively. In these tests, the output link of the actuation unit was locked mechanically against the mechanical end-stop. In addition, the system output impedance was assessed with the output link of the actuation unit free to move.

Step response: Twenty step signals of four different torque amplitudes ($\pm$ 0.5 Nm and $\pm$ 1 Nm) were commanded to the actuation unit, with a preload of $\pm$ 1.5 Nm for ensuring no detachment form the end-stop. For the stimulation at $\pm$ 0.5 Nm, the rise time was 0.02 ± 0.01 s, the settling time was 0.51 ± 0.20 s, and the overshoot was $21.9 \pm 23.20\%$. For the step at $\pm$ 1 Nm amplitude, the rise time was 0.02 ± 0.01 s, the settling time was 0.32 ± 0.08 s, and the overshoot was $25.65 \pm 5.02\%$. The mean responses over the twenty repetitions are shown in Fig. 3(a).

Chirp response: Three chirp signals were commanded to the actuation unit, spanning from 0.1 Hz to 6 Hz, with amplitudes of 0.5, 1, and 1.5 Nm with a with a preload of 2 Nm for ensuring no detachment from the end-stop. The transfer function $H(s) = \tau^{SEA}_{meas}(s)/\tau^{SEA}_{des}(s)$ was estimated from the data. Within the tested frequency range, the -3 dB cut-off frequency was not reached. The root-mean-squared error (RMSE) between the desired and the measured torque profiles was 0.29 ± 0.10 Nm over the three repetitions, with a phase lag of -18.25 deg at 1 Hz, -49.26 deg at 3 Hz, and -88.50 deg at 6 Hz. Results are presented in Fig. 3(a).

Output impedance: To compute the output mechanical impedance ($Z(s) = \tau^{SEA}_{meas}(s)/\dot{\theta}_{meas}(s)$), the actuation unit was set in TM ($\tau^{SEA}_{des} = 0$) and the output link was manually elicited by an experimenter trying to follow a chirp signal in a frequency range between 0.1 and 3.5 Hz. The mean amplitude of the Bode plot of $Z(s)$ ranged from 0.1 Nms/rad up to 0.25 Nms/rad over the explored frequency range (Fig. 3(b)).

Haptic rendering performance: The impedance control performance was evaluated in terms of the tracking error in following a reference angle trajectory. The two actuation units, E1 and E2, were put on the bench and configured in the *unidirectional interaction* control modality. Module E2 was set in TM and was manually moved by one experimenter to generate manually a chirp reference trajectory in a frequency range between 0.5 and 1 Hz. Module E1 was set in impedance control with a reference angle set on the measured joint angle of E2. The movement of E1 spanned a range of (0–112) deg. The angular RMSE between θ^{E2}_{meas} and θ^{E1}_{meas}, was 3.85 ± 1.49 deg, while the torque RMSE, computed between τ^{E1}_{des} and τ^{E1}_{meas} was 0.10 ± 0.06 Nm. The results are presented in (Fig. 3(c)).

IV. Human-in-the-Loop Experiments

The system performance was tested in a dyadic experiment, to assess whether the haptic feedback provided by the exoskeletons could be used to improve synchronization between the users in a rhythmic task. A hand-tapping task was chosen, in which subjects moved their elbow up and down while the visual and acoustic stimuli were suppressed.

A. Participants

Eight dyads (16 subjects, 10 males and 6 females, age 27.8 ± 2.7 years) were enrolled to participate in the experimental activity, which took place at The BioRobotics Institute of Scuola Superiore Sant'Anna (Pontedera, Pisa, Italy). Dyads were formed by pairing subjects with comparable height and weight, to ensure matching between the elbow kinematics and to minimize discrepancies in the perceived feedback caused by anthropometric differences. The experimental activities followed the principles stated in the declaration of Helsinki and all participants signed written informed consent before participating. The Institutional Review Board approved the experimental procedures (approval n. 39/2023).

B. Experimental Protocol

The experimental task consisted of performing a rhythmic hand-tapping gesture on a table surface through elbow F/E movements at a pace of 60 bpm (1 Hz). Upon arrival, the two subjects wore exoskeleton modules, and they were requested to sit on a chair with their elbows at around 90 deg and the upper arm lying along the body. The subjects were visually and acoustically isolated from each other using a panel obstructing the line of view and noise-reducing headphones (Fig. 4(a)). Additionally, they wore Bluetooth earphones (one single pair

Authorized licensed use limited to: Scuola Superio Sant'Anna di Pisa. Downloaded on August 27,2025 at 06:59:11 UTC from IEEE Xplore. Restrictions apply.

IEEE Robotics and Automation Letters (RA-L) paper, presented at ICRA 2026, Vienna, Austria. Cite as RA-L paper.

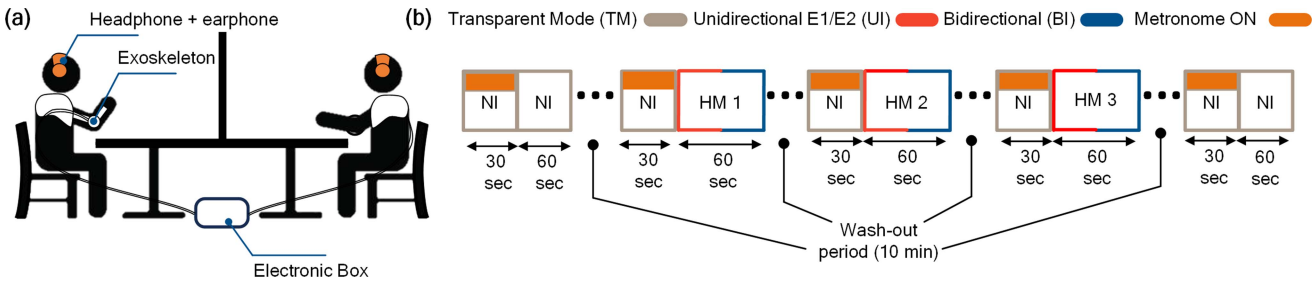

Fig. 4. (a) Experimental setup. The two subjects wear the exoskeleton modules and noise-reducing headphones. Wireless earphones are used to provide the metronome. (b) Five experimental blocks. Each block has a duration of 90 s and is composed of initial 30 s with the metronome turned on and exoskeletons set in TM, followed by 60 s with the metronome turned off. No Interaction (NI) conditions are tested always at the beginning and end of the experiment, whereas the haptic interactions (UI or BI) are randomized. A 10-minute wash-out period is placed between blocks.

shared by the two subjects) to listen to a metronome setting the pace of the movements. The experiment was composed of five blocks (Fig. 4(b)), each lasting 90 s. During the first 30 s, the subjects listened to the metronome to set a common reference rhythm; then the metronome was turned off and the participants were asked to maintain the pace for 60 s. After each block, a 10-minute wash-out period was added, similar to [29]. The first and the last block were performed in no interaction mode (called NI Start and NI End). The remaining three blocks were randomized to set the modules in unidirectional mode (UI, with E1 set as the *leader* and E2 as the *follower*, and vice versa) and bidirectional mode (BI). The NI blocks were not randomized to allow for investigation of potential retention effects from the exposure to the feedback. The subjects were blinded to the different experimental conditions to reduce bias effects.

C. Data Analysis and Statistics

Collected data were analyzed using MATLAB 2022b (The MathWorks, Natick, MA, USA). All metrics were extracted from the data collected in the last 60 s of each block and then aggregated between subjects. For each dyad and condition, the RMSE between the measured elbow angle trajectories collected from the two exoskeletons was computed. Limit cycle analysis was conducted to estimate the movement phase ($\phi_{E_{n|1,2}}$) using the state-space method. The phase was computed in the phase plane as a function of the rotating vectors:

$$\phi_{E_{n|1,2}} = \tan^{-1}\left(\dot{\theta}_{E_n}/\theta_{E_n}\right) \tag{4}$$

where θ_{E_n} and $\dot{\theta}_{E_n}$ are respectively the angle trajectory and the speed trajectory of E1 or E2. The phase difference between the two signals was computed in absolute value:

$$|\Delta\phi| = |\phi_{E_1} - \phi_{E_2}| \tag{5}$$

Additionally, the Euclidian distance (d_c) was estimated between the two centroids of the limit cycles, computed as mean values of angle and speed profiles in the phase plane for the different haptic conditions:

Where $(\bar{\theta}_{E_n}, \bar{\dot{\theta}}_{E_n})$ represents the mean values (centroids) of the trajectories in the angle vs speed phase plane. The two variables were normalized using min-max normalization across conditions, resulting in a value between 0 and 1. The maximum and minimum values for angles and speeds for each condition were observed to assess variations between the different haptic conditions. Statistical analysis was conducted to evaluate differences in the five different blocks for all metrics. The normality of the computed metrics' distribution was assessed using the Shapiro-Wilks test. Since data were found not normally distributed, a non-parametric one-way analysis of variance (Friedman test) was applied to check for differences across the five blocks. Then, when appropriate, post-hoc comparisons were carried out through the Tukey-Kramer correction. All statistical analyses were conducted in MATLAB 2022b using a significance level $\alpha = 5\%$. Moreover, two metrics were computed, namely the median of the absolute peak torque recorded during the trial (*Me* ($|\tau_{pks}|$)) [19] and the RMSE between the desired and measured torque profiles. The RMSE was analyzed to determine whether the overall controller error during operation conditions exceeded the threshold for perceived torque, potentially introducing a bias in the perceived interaction if it overcome the just noticeable difference (JND) of 0.2 Nm for the haptic feedback at the elbow level [24]. Both metrics were computed in the UI and BI blocks, while RMSE was also computed in the NI blocks.

D. Results

Experimental results are shown in Fig. 5. The RMSE between the two elbow trajectories (Fig. 5(a)) in the BI block was significantly lower than in the initial NI of around 52.10% (p = 1.4e-3) and the final NI block of around 57.21% (p = 1.9e-4). On average, the UI blocks resulted in lower error compared to the initial and final NI blocks (reductions were 36.84% and 43.60%, respectively), with a significance of the UI-E1 block ($p = 0.014$) and a trend towards significance in UI-E2 block ($p = 0.084$). No significant differences were observed between the BI and the two UI blocks ($p = 0.712$ and $p = 0.408$), between the two UI blocks ($p = 0.989$), or between the two NI ones ($p = 0.987$). Similarly, the $|\Delta\phi|$ (Fig. 5(b)) computed in the BI block exhibited significantly smaller values compared to both the first and last NI blocks, with a reduction of approximately 61.37% ($p = 0.022$). Likewise, in the UI blocks, median values decreased by 53.55% for E1 and 42.01% for E2 relative to the NI blocks. The reduction was statistically significant for E1 (p = 0.014) and showed a trend toward significance for E2 (p = 0.056). No significant differences were observed between either UI blocks ($p = 0.989$) or the two NI ones ($p = 0.803$). Concerning the d_c values (Fig. 5(c)), the Friedman test showed no significant difference among the conditions ($p = 0.240$). The maximum and minimum elbow's angles were 111.5 (104.3–115.0) deg and 66.4 (62.5–67.5) deg, with a median variation < 1 deg across conditions. The maximum speed values were recorded during

Authorized licensed use limited to: Scuola Superio Sant'Anna di Pisa. Downloaded on August 27,2025 at 06:59:11 UTC from IEEE Xplore. Restrictions apply.

IEEE Robotics and Automation Letters (RA-L) paper, presented at ICRA 2026, Vienna, Austria. Cite as RA-L paper.

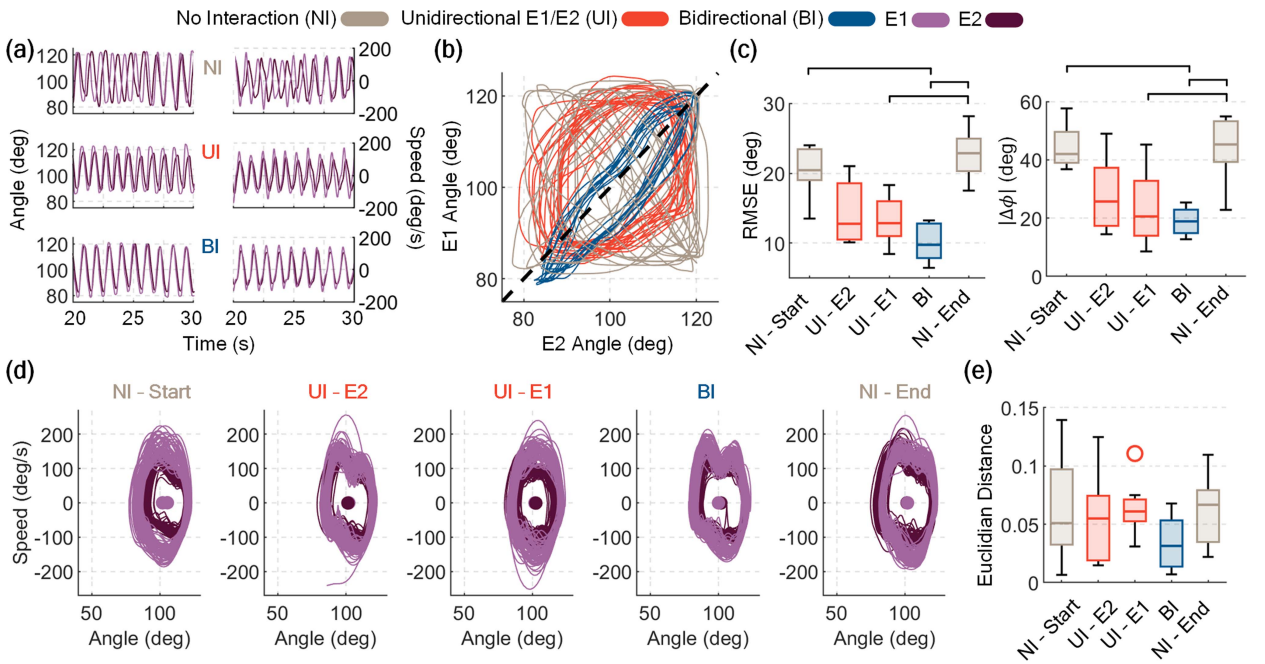

Fig. 5. Experimental results. (a) Time series of the elbow angle and speed of a representative dyad. (b) Elbow angles of a representative dyad in the angle-angle plot. (c) Boxplots of the RMSE between E1 and E2 trajectories for the different conditions and the phase difference between E1 and E2 in the different conditions across subjects. (d) Representative results of a dyad for the limit cycle analysis in the phase plane (speed/angle relation). (e) Aggregated results for the Euclidian distance of the centroids in each condition. Statistically significant differences ($p<0.05$) are indicated with horizontal bars.

TABLE I
MEDIAN OF THE PEAK TORQUE ($ME(|\tau_{pks}|)$,) AND RMSE REPORTED FOR EACH FEEDBACK CONDITIONS

	Me **($\|\tau_{pks}\|$) (Nm)**		**RMSE (Nm)**	
	E1	E2	E1	E2
NI Start	-	-	0.23 (0.20-25)	0.22 (0.20-0.25)
UI E2	-	0.88 (0.57-1.32)	0.22 (0.20-0.23)	0.24 (0.22-0.31)
UI E1	1.06 (0.96-1.13)	-	0.26 (0.22-0.28)	0.21 (0.20-0.28)
BI	0.92 (0.84-1.09)	0.73 (0.61-0.90)	0.26 (0.22-0.29)	0.26 (0.20-0.29)
NI End	-	-	0.21 (0.18-0.23)	0.20 (0.18-0.22)

All the values are reported as median (IQR).

the NI condition, with a median of 195.2 (177.5–201.2) deg/s. The median value decreased to 185.10 (176.4–195.6) deg/s with the haptic bidirectional and unidirectional feedback. The median torque RMSE across all conditions was 0.23 (0.18–0.31) Nm, with no major deviation between the NI mode and the haptic feedback conditions. The median absolute peak torques reached a median value of 0.88 and 1.06 Nm during the UI condition, while in the BI these values were reduced by 17% and 13% respectively for E2 and E1. The *Me* ($|\tau_{pks}|$) and RMSE torque values for each condition are reported Table I.

V. DISCUSSIONS

A. Mechatronics Design Performance

This work presented the development of an elbow exoskeleton based on SEA architecture, exploited as a tool for studying haptic interaction between two human agents. The resulting system features a compact and lightweight structure, with a weight in line with other state-of-the-art devices [23], [30], while preserving the advantages of a rigid-structure-based exoskeleton and maintaining an advantageous weight-to-power ratio. The control system showed adequate performance for rendering haptic feedback in terms of closed-loop torque bandwidth (6 Hz compared to the functional requirement of 1.2 Hz) [18] and transparency (residual torque in TM in the range of the JND of 0.2 Nm). The mechanical output impedance in TM was 0.25 Nms/rad at a frequency of 3.5 Hz, and below 0.1 Nms/rad for the frequency requested during the tapping movement (1 Hz). This finding demonstrates the device's suitability for applications involving movement kinematics that accommodate physiological motions [22]. The torque tracking RMSEs with haptic feedback were close to the JND and comparable to values reported for similar platforms [31]. Thus, the exoskeleton demonstrated its ability to provide feedback with an error range negligible for the intended application scenario. Overall, the system demonstrates a feasible high-quality haptic interface for the targeted application.

B. Dyadic Synchronization Scenario

Several studies have examined the application of visual, auditory and haptic vibrotactile feedback for improving the relative phase synchronization between users [6]. However, this exteroceptive information are limited in scenarios where the user is performing an attention-demanding and structured task [32]. In this study, haptic feedback provided through a wearable device was used to actively modify the user behavior in a rhythmic task, improving the overall synchronization between two participants. Indeed, the results suggest that the information provided by the exoskeleton was successfully integrated into the

Authorized licensed use limited to: Scuola Superio Sant'Anna di Pisa. Downloaded on August 27,2025 at 06:59:11 UTC from IEEE Xplore. Restrictions apply.

IEEE Robotics and Automation Letters (RA-L) paper, presented at ICRA 2026, Vienna, Austria. Cite as RA-L paper.

user's sensorimotor scheme, even if the subjects were unaware of the exposed feedback condition. The low RMSE between the two joint trajectories (median value always below 15 deg) and the low relative phase delay between the taps (median value always below 30 deg) suggest an alignment of the users' movements when the haptic feedback was active, especially in the BI condition. Notably, these results were similar to the ones observed in previous studies in which exteroceptive feedback modalities, e.g., audio-visual stimuli, were tested in similar tasks [33], [34]. These findings suggest that exoskeletons could be used to synchronize the users' actions using a direct proprioceptive feedback, which could be also useful in reducing the cognitive load compared to exteroceptive modalities [35]. Indeed, exoskeletons bypass the need for the cognitive interpretation of the feedback by providing a direct haptic sensation to the motor system [36]. Notably, a statistically significant increasing trend in the median RMSE and phase error values was observed comparing the final NI block to the tested haptic conditions. Although the experimental protocol was designed to minimize fatigue and habituation, this might suggest some motor learning outcomes thanks to dyad interaction rendered via the exoskeletons. Additionally, while all haptic conditions were successful in enhancing the synchronization between partners, the BI condition was far more effective in conveying the relative motion information, as reflected by the overall increased synchrony compared to both the initial and final NI blocks. Therefore, a collaborative paradigm may be more beneficial in achieving the task goal compared to a cooperative (*leader-follower*) one, as previously investigated in [37]. Moreover, in terms of the overall shape of the movement in the phase plane, the centroids' positions showed a substantial tendency towards alignment in BI condition compared to the NI and UI ones, albeit not significant. This could suggest an increased relative coordination between the two subjects in BI condition. Overall, the shape of the limit cycle plot in terms of angle and speed amplitude was preserved during haptic conditions, thus demonstrating that the feedback was effective and did not alter the kinematic features of the gesture, showing only a limited reduction in the average speed ($<$10 deg/s). This reduction can be explained by neuroscientific principles, as users could have initially perceived the haptic feedback as a disturbance to their internal rhythm introduced by an external one, i.e., the one of the paired subjects [38]. The resulting emergent rhythm is therefore a tradeoff between the cognitive effort in interpreting the feedback, translating the perceived stimuli in a coherent motor outcome, and the goal of maintaining a pace consistent with the metronome [37].

Some limitations can be pointed out in the current version of the study. First, despite the encouraging results obtained regarding technical performance, a larger participant pool is essential to reinforce the preliminary findings and draw more conclusive evidence on feedback interpretability. Increasing the sample size is critical to distinguish more clearly the relative effectiveness of unidirectional versus bidirectional feedback in conveying timing information. In addition, this preliminary study did not include a questionnaire to capture subjective feedback. Future assessments of the feedback strategy and overall device performance would significantly benefit from integrating subjective measures of task dominance, such as the Self-Assessment Manikin (SAM), to yield deeper insights into user experience and perceived effectiveness. When looking for possible short-term adaptation effects, no significant differences were found between the initial and final NI conditions. This outcome reflects the limited feedback exposure, adequate washout duration, and low complexity of the task, which was not expected to yield significant learning gains [39]. Increasing task complexity, e.g., by adding more degrees of freedom, would be a logical next step. However, validating the results on a single joint was essential before extending the approach to multi-joint tasks such as musical performance, sports, or other collaborative activities. In addition, the study was designed without a control group nor a control condition, such as audio or visual feedback. Although the results are in line with other state-of-the-art works, a general conclusion compared to other feedback modalities falls beyond the scope of this work. Lastly, this study did not explore the impact of exoskeleton feedback on muscle co-contraction. Investigating this aspect could provide valuable insights for developing targeted feedback strategies aimed at enhancing movement smoothness and task accuracy [40], by accelerating the formation of the internal model of the gesture even when the overall kinematics and dynamics are rather fast [41]. Nevertheless, the findings of this study suggest that the device can be effectively used in HRH interaction scenarios, such as playing musical instruments like drums or violin, where individuals are learning new gestures or professionals are refining their skills, particularly to overcome the ceiling effect described in [42]. In such scenarios, pairing experienced individuals (teachers) with novices (learners) may enhance motor learning by engaging an alternative sensory channel enabled by this technology. Extensions of the present work would tackle the mentioned limitations, especially focusing on investigating learning effects and increasing the complexity of the motor task, assessing the retention after exposure to the stimuli. In addition, the use of biological signals and adaptive control strategies to tune and improve communication between the two users should be considered, aiming to enhance the tuning of the stimulus to the subject's performance. Finally, future validation will be conducted in realistic, unstructured scenarios, such as violin playing, to demonstrate the practical effectiveness of the technology.

REFERENCES

[1] T. Ceux, M. J. Buekers, and G. Montagne, "The effects of enhanced visual feedback on human synchronization," *Neurosci. Lett.*, vol. 349, no. 2, pp. 103–106, Oct. 2003, doi: 10.1016/S0304-3940(03)00799-7.

[2] T. Lorenz, A. Mortl, B. Vlaskamp, A. Schubo, and S. Hirche, "Synchronization in a goal-directed task: Human movement coordination with each other and robotic partners," in *Proc. 2011 Robot Hum. Interactive Commun.*, Atlanta, GA, USA, Jul. 2011, pp. 198–203, doi: 10.1109/ROMAN.2011.6005253.

[3] A. Mörtl, T. Lorenz, B. N. S. Vlaskamp, A. Gusrialdi, A. Schubö, and S. Hirche, "Modeling inter-human movement coordination: Synchronization governs joint task dynamics," *Biol. Cybern.*, vol. 106, no. 4–5, pp. 241–259, Jul. 2012, doi: 10.1007/s00422-012-0492-8.

[4] D. C. Comstock, M. J. Hove, and R. Balasubramaniam, "Sensorimotor synchronization with auditory and visual modalities: Behavioral and neural differences," *Front. Comput. Neurosci.*, vol. 12, Jul. 2018, Art. no. 53, doi: 10.3389/fncom.2018.00053.

[5] E. Ivanova, J. Eden, G. Carboni, J. Krüger, and E. Burdet, "Interaction with a reactive partner improves learning in contrast to passive guidance," *Sci. Reports*, vol. 12, no. 1, Sep. 2022, Art. no. 15821, doi: 10.1038/s41598-022-18617-7.

[6] R. Sigrist, G. Rauter, R. Riener, and P. Wolf, "Augmented visual, auditory, haptic, and multimodal feedback in motor learning: A review," *Psychon. Bull Rev.*, vol. 20, no. 1, pp. 21–53, Feb. 2013, doi: 10.3758/s13423-012-0333-8.

[7] M. R. Short et al., "Haptic human-human interaction during an ankle tracking task: Effects of virtual connection stiffness," *IEEE Trans. Neural Syst. Rehabil. Eng.*, vol. 31, pp. 3864–3873, 2023, doi: 10.1109/TNSRE.2023.3319291.

Authorized licensed use limited to: Scuola Superio Sant'Anna di Pisa. Downloaded on August 27,2025 at 06:59:11 UTC from IEEE Xplore. Restrictions apply.

IEEE Robotics and Automation Letters (RA-L) paper, presented at ICRA 2026, Vienna, Austria. Cite as RA-L paper.

[8] R. Lokesh et al., "Visual accuracy dominates over haptic speed for state estimation of a partner during collaborative sensorimotor interactions," *J. Neurophysiol.*, vol. 130, no. 1, pp. 23–42, Jul. 2023, doi: 10.1152/jn.00053.2023.

[9] T. Koritnik, A. Koenig, T. Bajd, R. Riener, and M. Munih, "Comparison of visual and haptic feedback during training of lower extremities," *Gait Posture*, vol. 32, no. 4, pp. 540–546, Oct. 2010, doi: 10.1016/j.gaitpost.2010.07.017.

[10] E. B. Küçüktabak, S. J. Kim, Y. Wen, K. Lynch, and J. L. Pons, "Human-machine-human interaction in motor control and rehabilitation: A review," *J. NeuroEng. Rehabil.*, vol. 18, no. 1, Dec. 2021, Art. no. 183, doi: 10.1186/s12984-021-00974-5.

[11] P. K. Mathavan Jeyabalan, A. Nehrujee, S. Elias, M. M. Kumar, S. Sujatha, and S. Balasubramanian, "Design and characterization of a self-aligning end-effector robot for single-joint arm movement rehabilitation," *Robotics*, vol. 12, no. 6, Nov. 2023, Art. no. 149, doi: 10.3390/robotics12060149.

[12] A. Noccaro, S. Buscaglione, M. Pinardi, G. Di Pino, and D. Formica, "Evaluation of a 7-DoFs robotic manipulator as haptic interface during planar reaching tasks," in *Proc. 2023 IEEE/RSJ Int. Conf. Intell. Robots Syst.*, Detroit, MI, USA, Oct. 2023, pp. 5095–5100, doi: 10.1109/IROS55552.2023.10342470.

[13] F. Bernardoni, O. Ozen, K. Buetler, and L. Marchal-Crespo, "Virtual reality environments and haptic strategies to enhance implicit learning and motivation in robot-assisted training," in *Proc. IEEE 16th Int. Conf. Rehabil. Robot.*, Toronto, ON, Canada, Jun. 2019, pp. 760–765, doi: 10.1109/ICORR.2019.8779420.

[14] L. Vianello et al., "Exoskeleton-mediated physical Human-Human interaction for a sit-to-stand rehabilitation task," in *Proc. IEEE Int. Conf. Robot. Automat.*, Yokohama, Japan, 2024, doi: 10.1109/ICRA57147.2024.10610796.

[15] E. B. Küçüktabak, Y. Wen, M. Short, E. Demirbaş, K. Lynch, and J. Pons, "Virtual physical coupling of two lower-limb exoskeletons," in *Proc. 2023 Int. Conf. Rehabil. Robot.*, Singapore, Sep. 2023, pp. 1–6, doi: 10.1109/ICORR58425.2023.10304601.

[16] Z. Li, G. Li, X. Wu, Z. Kan, H. Su, and Y. Liu, "Asymmetric cooperation control of dual-arm exoskeletons using human collaborative manipulation models," *IEEE Trans. Cybern.*, vol. 52, no. 11, pp. 12126–12139, Nov. 2022, doi: 10.1109/TCYB.2021.3113709.

[17] M. A. Gull, S. Bai, and T. Bak, "A review on design of upper limb exoskeletons," *Robotics*, vol. 9, no. 1, Mar. 2020, Art. no. 16, doi: 10.3390/robotics9010016.

[18] A. Gupta and M. K. O'Malley, "Design of a haptic arm exoskeleton for training and rehabilitation," *IEEE/ASME Trans. Mechatron.*, vol. 11, no. 3, pp. 280–289, Jun. 2006, doi: 10.1109/TMECH.2006.875558.

[19] J. Pan et al., "NESM- γ : An upper-limb exoskeleton with compliant actuators for clinical deployment," *IEEE Robot. Autom. Lett.*, vol. 7, no. 3, pp. 7708–7715, Jul. 2022, doi: 10.1109/LRA.2022.3183926.

[20] S. Fornalski, R. Gupta, and T. Q. Lee, "Anatomy and biomechanics of the elbow joint," *Techn. Hand Upper Extremity Surg.*, vol. 7, no. 4, pp. 168–178, 2003.

[21] "CONnected through roBOTS: Physically coupling humans to boost handwriting and music learning | CONBOTS | Project | fact Sheet | H2020 | CORDIS | European commission," Accessed: May 05, 2025. [Online]. Available: https://cordis.europa.eu/project/id/871803

[22] N. Vitiello et al., "NEUROExos: A powered elbow exoskeleton for physical rehabilitation," *IEEE Trans. Robot.*, vol. 29, no. 1, pp. 220–235, Feb. 2013, doi: 10.1109/TRO.2012.2211492.

[23] M. Xiloyannis, L. Cappello, K. D. Binh, C. W. Antuvan, and L. Masia, "Preliminary design and control of a soft exosuit for assisting elbow movements and hand grasping in activities of daily living," *J. Rehabil. Assistive Technol. Eng.*, vol. 4, Jan. 2017, Art. no. 205566831668031, doi: 10.1177/2055668316680315.

[24] H. Kim and A. T. Asbeck, "Just noticeable differences for elbow joint torque feedback," *Sci. Reports*, vol. 11, no. 1, Dec. 2021, Art. no. 23553, doi: 10.1038/s41598-021-02630-3.

[25] I. A. Murray and G. R. Johnson, "A study of the external forces and moments at the shoulder and elbow while performing every day tasks," *Clin. Biomech.*, vol. 19, no. 6, pp. 586–594, Jul. 2004, doi: 10.1016/j.clinbiomech.2004.03.004.

[26] M. M. White, O. N. Morejon, S. Liu, M. Y. Lau, C. S. Nam, and D. B. Kaber, "Muscle loading in exoskeletal orthotic use in an activity of daily living," *Appl. Ergonom.*, vol. 58, pp. 190–197, Jan. 2017, doi: 10.1016/j.apergo.2016.06.010.

[27] A. Mazzarini et al., "A model-based framework for the selection of mechatronic components of wearable robots: Preliminary design of an active ankle-foot prosthesis," in *Computers Helping People With Special Needs*, K. Miesenberger, G. Kouroupetroglou, K. Mavrou, R. Manduchi, M. Covarrubias Rodriguez, and P. Penáz, Eds. Cham, Switzerland: Springer, 2022, pp. 453–460, doi: 10.1007/978-3-031-08645-8_53.

[28] A. Baldoni, M. Fantozzi, and N. Vitiello, "A planar torsional spring," US Patent WO2020104962A1, 2018. [Online]. Available: https://patents.google.com/patent/US20220003292A1/en

[29] S. J. Kim et al., "A framework for dyadic physical interaction studies during ankle motor tasks," *IEEE Robot. Autom. Lett.*, vol. 6, no. 4, pp. 6876–6883, Oct. 2021, doi: 10.1109/LRA.2021.3092265.

[30] H. H. Cheng, T. M. Kwok, and H. Yu, "Design and control of the portable upper-limb elbow-forearm exoskeleton for ADL assistance," in *Proc. 2023 IEEE/ASME Int. Conf. Adv. Intell. Mechatron.*, Seattle, WA, USA, Jun. 2023, pp. 343–349, doi: 10.1109/AIM46323.2023.10196165.

[31] T. Chen, R. Casas, and P. S. Lum, "An elbow exoskeleton for upper limb rehabilitation with series elastic actuator and cable-driven differential," *IEEE Trans. Robot.*, vol. 35, no. 6, pp. 1464–1474, Dec. 2019, doi: 10.1109/TRO.2019.2930915.

[32] C. E. Proulx, M. T. Louis Jean, J. Higgins, D. H. Gagnon, and N. Dancause, "Somesthetic, visual, and auditory feedback and their interactions applied to upper limb neurorehabilitation technology: A narrative review to facilitate contextualization of knowledge," *Front. Rehabil. Sci.*, vol. 3, Mar. 2022, Art. no. 789479, doi: 10.3389/fresc.2022.789479.

[33] I. Konvalinka, P. Vuust, A. Roepstorff, and C. D. Frith, "Follow you, Follow me: Continuous mutual prediction and adaptation in joint tapping," *Quart. J. Exp. Psychol.*, vol. 63, no. 11, pp. 2220–2230, Nov. 2010, doi: 10.1080/17470218.2010.497843.

[34] M. Roerdink, C. E. Peper, and P. J. Beek, "Effects of correct and transformed visual feedback on rhythmic visuo-motor tracking: Tracking performance and visual search behavior," *Hum. Movement Sci.*, vol. 24, no. 3, pp. 379–402, Jun. 2005, doi: 10.1016/j.humov.2005.06.007.

[35] C. Provenzale, F. Di Tommaso, N. Di Stefano, D. Formica, and F. Taffoni, "Real-time visual feedback based on MIMUs technology reduces bowing errors in beginner violin students," *Sensors*, vol. 24, no. 12, Jun. 2024, Art. no. 3961, doi: 10.3390/s24123961.

[36] S. J. Sober and P. N. Sabes, "Multisensory integration during motor planning," *J. Neurosci.*, vol. 23, no. 18, pp. 6982–6992, Aug. 2003, doi: 10.1523/JNEUROSCI.23-18-06982.2003.

[37] W. Gomes, P. Maurice, J. Babič, J.-B. Mouret, and S. Ivaldi, "In a collaborative Co-manipulation, humans have a motor behaviour similar to a leader," hal-03573469, 2022. [Online]. Available: https://hal.science/hal-03573469

[38] A. Takagi, F. Usai, G. Ganesh, V. Sanguineti, and E. Burdet, "Haptic communication between humans is tuned by the hard or soft mechanics of interaction," *PLoS Comput. Biol.*, vol. 14, no. 3, Mar. 2018, Art. no. e1005971, doi: 10.1371/journal.pcbi.1005971.

[39] E. Basalp, P. Wolf, and L. Marchal-Crespo, "Haptic training: Which types facilitate (re)learning of which motor task and for whom? Answers by a review," *IEEE Trans. Haptics*, vol. 14, no. 4, pp. 722–739, Oct. 2021, doi: 10.1109/TOH.2021.3104518.

[40] P. L. Gribble, L. I. Mullin, N. Cothros, and A. Mattar, "Role of cocontraction in arm movement accuracy," *J. Neurophysiol.*, vol. 89, no. 5, pp. 2396–2405, May 2003, doi: 10.1152/jn.01020.2002.

[41] J. B. Heald, D. W. Franklin, and D. M. Wolpert, "Increasing muscle co-contraction speeds up internal model acquisition during dynamic motor learning," *Sci. Reports*, vol. 8, no. 1, Nov. 2018, Art. no. 16355, doi: 10.1038/s41598-018-34737-5.

[42] S. Furuya, T. Oku, H. Nishioka, and M. Hirano, "Surmounting the ceiling effect of motor expertise by novel sensory experience with a hand exoskeleton," *Sci. Robot.*, vol. 10, no. 98, Jan. 2025, Art. no. eadn3802, doi: 10.1126/scirobotics.adn3802.

Authorized licensed use limited to: Scuola Superio Sant'Anna di Pisa. Downloaded on August 27,2025 at 06:59:11 UTC from IEEE Xplore. Restrictions apply.